Bioinformatics, 34, 2018, i781–i786
doi: 10.1093/bioinformatics/bty556
ECCB 2018

OXFORD

Insights on the alteration of functionality of a tyrosine kinase 2 variant: a molecular dynamics study

Nastazia Lesgidou[1], Elias Eliopoulos[2], George N. Goulielmos[3] and Metaxia Vlassi[1,*]

[1]Laboratory of Protein Structure & Molecular Modeling, Institute of Biosciences & Applications, National Center for Scientific Research "DEMOKRITOS", Athens 15310, Greece, [2]Laboratory of Genetics, Department of Biotechnology, Agricultural University of Athens, Athens 11855, Greece and [3]Section of Molecular Pathology and Human Genetics, Department of Internal Medicine, School of Medicine, University of Crete, Heraklion 71003, Greece

*To whom correspondence should be addressed.

Abstract

Motivation: The tyrosine kinase 2 protein (Tyk2), encoded by the *TYK2* gene, has a crucial role in signal transduction and the pathogenesis of many diseases. A single nucleotide polymorphism of the *TYK2* gene, SNP rs34536443, is of major importance, since it has been shown to confer protection against various, mainly, autoimmune diseases. This polymorphism results in a Pro to Ala change at amino acid position 1104 of the encoded Tyk2 protein that affects its enzymatic activity. However, the details of the underlined mechanism are unknown. To address this issue, in this study, we used molecular dynamics simulations on the kinase domains of both wild type and variant Tyk2 protein.

Results: Our MD results provided information, at atomic level, on the consequences of the Pro1104 to Ala substitution on the structure and dynamics of the kinase domain of Tyk2 and suggested reduced enzymatic activity of the resulting protein variant due to stabilization of inactive conformations, thus adding to knowledge towards the elucidation of the protection mechanism against autoimmune diseases associated with this point mutation.

Contact: meta@bio.demokritos.gr

1 Introduction

The tyrosine kinase 2 (Tyk2) protein encoded by the *TYK2* gene, is a member of the Janus kinases (JAK) family with a crucial role for signal transduction in response to various cytokines, including type I interferon (IFN) as well as proinflammatory and anti-inflammatory cytokines (Langrish *et al.*, 2004; Murray, 2007; Shimoda *et al.*, 2000; Velazquez *et al.*, 1992). Tyk2 is part of the STAT signaling pathway and binds to the type I interferon-a receptor (IFNAR) on the cell surface of IFN-producing cells, thus playing a major role in the pathogenesis of various autoimmune and inflammatory diseases (Kyogoku and Tsuchiya, 2007).

Each of the four JAK proteins consists of a large amino-terminal region, a pseudo-kinase domain and a catalytic domain (or kinase domain). The phosphorylation of the kinase domain (KD) is the activation switch of these kinases (Yamaoka *et al.*, 2004). Various crystal structures of Tyk2 domains have been determined [e.g. crystal structure of an ADP-bound form of its KD; PDB entry code: 4GVJ (Liang *et al.*, 2013), Fig. 1]. The 3D-structure of the KD segment of Tyk2 is divided in two structurally distinct regions, characteristic of protein kinases: the N-terminal lobe (residues: 889–979) and the C-terminal lobe (residues: 985–1176) (Fig. 1). The active site of the protein is located at the crevice created between the two lobes.

The activation segment of Tyk2 (A-loop), located at the beginning of its C-terminal lobe, contains two sequential tyrosine residues (Y1054, Y1055; Fig. 1), phosphorylation of which is necessary for the activation of this protein (Gauzzi *et al.*, 1996) and subsequent activation of the signaling pathway (Lucet *et al.*, 2006).

Tyk2 is encoded by the *TYK2* gene located on chromosome 19p13.2 (Lindqvist *et al.*, 2000). Polymorphisms of the *TYK2* gene have been recently found to be associated with various autoimmune diseases as well as endometriosis (Peluso *et al.*, 2013). One of these polymorphisms, namely the single nucleotide polymorphism (SNP), rs34536443 is of particular importance since it has been shown to confer protection against several autoimmune diseases, such as: Multiple Sclerosis (Dyment *et al.*, 2012), Psoriatic Arthritis (Myrthianou *et al.*, 2017), Rheumatoid Arthritis, Systemic Lupus

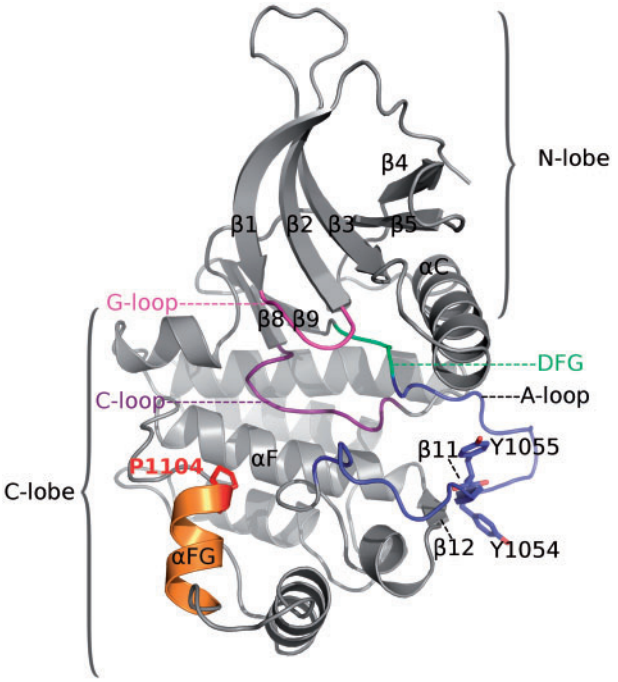

Fig. 1. 3D-structure of the kinase domain of Tyk2. Ribbon model representation, rendered using coordinates from a known crystal structure [PDB entry code: 4GVJ (Liang *et al.*, 2013)]. β-Strands and α-helices are shown as arrows and ribbons, respectively. Various structural elements and regions corresponding to characteristic features of JAK kinases are shown in color and indicated. Proline 1104 and important for activation tyrosine residues discussed in the text are labeled and shown as stick models

Erythematosus and Inflammatory Bowel diseases (Diogo *et al.*, 2015), as well as protection against endometriosis (Peluso *et al.*, 2013). This polymorphism results in a Pro1104 (Fig. 1) to Ala substitution in the amino acid sequence of the Tyk2 protein and has been shown to affect the enzymatic activity of this protein and therefore the associated cytokine pathways (Couturier *et al.*, 2011; Tomasson *et al.*, 2008). However the atomic details of the underlined mechanism of this, remain unknown.

In this study, we used molecular dynamics simulations, to address this issue.

2 Methods

The molecular dynamics simulations (MD) were performed on the KD domains of both, variant (P1104A hereafter) and wild type Tyk2 (wtTyk2 hereafter) using the GROMACS software package (Hess *et al.*, 2008). The known crystal structure of the ADP-bound form of wtTyk2 [from the Protein Data Bank entry: 4GVJ (Liang *et al.*, 2013); only protein atoms were extracted] and a 3D-model we constructed by *in-silico* mutagenesis using the VMD program (Humphrey *et al.*, 1996), were used as initial conformations of wtTyk2 and the P1104A variant, respectively. The MD simulations were carried out in explicit water using the gromos96 53a6 force field (Oostenbrink *et al.*, 2004). Periodic dodecahedron boxes of SPC water molecules (Berendsen *et al.*, 1987) extending 10 Å from protein atoms were used to solvate the protein systems, which were subsequently neutralized with counter-ions and optimized by steepest descent energy minimization. Energy optimization was followed by restrained MD simulations where the protein atoms were harmonically restrained to their initial position to allow the solvent to equilibrate. The equilibration step (for a total of 200 ps) was performed for 100 ps under the NVT conditions followed by 100 ps in the NPT ensemble. The temperature and pressure of the systems were kept constant, at 300 K and 1 bar, respectively. The optimization phase was followed by unrestrained MD simulations (MD production runs) in the NPT ensemble. A cut-off radius of 10 Å was employed for all non-bonded interactions in all MD simulations. To overcome sampling problems, multiple (three for each), independent, 100 ns-long MD simulations were carried out for both wtTyk2 and P1104A. The replicas were produced using different, random sets of starting velocities for the atoms. A similar procedure we used in (Voukkalis *et al.*, 2016).

MD analyses were based on various metrics and were performed on the respective MDs of each protein under study, both separately and on average within their sets of MD trajectories.

Convergence of the MD trajectories was assessed by monitoring the root-mean-square deviation (RMSD) of all the backbone atoms from the initial structure, along the MD trajectories.

The conformational flexibility of both proteins during their corresponding MD trajectories was assessed by means of root mean square fluctuation (RMSF) calculations. The RMSF values are a measure of atomic fluctuations along an MD trajectory and were calculated using the equation:

$$\mathrm{RMSF} = \sqrt{\langle \Delta r^2 \rangle_t}, \quad (1)$$

where Δr is the instantaneous fluctuation (displacement) of the position of an atom (or set of atoms) relative to its mean position and $<>_t$. denotes simulation time averaged values over the MD trajectory. RMSF values were calculated after superimposing each individual structure of a trajectory onto the initial structure by means of least-squares fitting, to remove rotational and translational motions. In this study, RMSF calculations were performed on the backbone atoms of wtTyk2 and P1104A for the last 40 ns of the corresponding 100-ns MD trajectories, both separately and on average within each set of three MD trajectories. A similar analysis we used previously in (Voukkalis *et al.*, 2016). Atomic fluctuations were also represented as temperature factors (B-factor), which are related to atomic fluctuations according to:

$$\mathrm{B-factor} = 8\pi^2 \langle \Delta r^2 \rangle_t,$$

The dominant modes of protein's motions were calculated by means of principal component analysis (PCA). PCA or covariance analysis is a statistical method used to identify the most relevant collective motions along MD trajectories (Amadei *et al.*, 1993). PCA uses the covariance matrix of atomic coordinates, the elements of which are defined as:

$$\mathrm{Cov}_{ij} = \langle \Delta \mathbf{r}_i \, \Delta \mathbf{r}_j \rangle_t, \quad (2)$$

where $\Delta \mathbf{r}_i$ and $\Delta \mathbf{r}_j$ are the vectors of the instantaneous fluctuation of the position of atoms i and j, relative to their mean positions and $<>_t$. denotes time averaged values over the MD trajectory. Diagonalization of the covariance matrix produces a set of eigenvectors, each defined by an eigenvalue, corresponding to directions and amplitudes of collective motions. Thus, PCA allows elimination of the noise from the dominant modes of system motions (Amadei *et al.*, 1993). In the present study, PCA was performed on the backbone atoms of wtTyk2 and P1104A along their respective single 120-ns trajectories generated by the concatenation of the last 40 ns of their respective sets of three100-ns MD simulations.

The extent of correlation of the motions of various parts of both proteins under study was examined via the calculation of cross-correlation matrices. The elements of the correlation matrix, namely the correlation coefficients, $Corr_{i,j}$ between two atoms i and j, are defined by the equation:

$$Corr_{i,j} = Cov_{i,j} / \sqrt{\langle \Delta r_i^2 \rangle \langle \Delta r_j^2 \rangle}_t,$$

with terms defined as in Equations (1) and (2).

Cross-correlation maps allow identification of residues moving collectively either in the same or in opposite directions (correlation coefficient values close to +1, or −1, respectively) along MD trajectories. In the present study, cross-correlation coefficients were calculated for the motions of all the C^{α} atoms of both wtTyk2 and P1104A along their respective concatenated MD trajectories (see above). The 120-ns single trajectories were also used for the corresponding backbone B-factor estimations and structure averaging. RMSF calculations, structure averaging, B-factor estimations and PCA analyses were carried out using related analysis tools of GROMACS, whereas cross-correlation analysis was performed using a related GROMACS tool modified accordingly, in house (C. Zarkadas and M. Vlassi, IB-A, NCSR 'Demokritos', unpublished).

Secondary structure analyses made use of the DSSP algorithm (Kabsch and Sander, 1983) and were performed along all the 100-ns MD trajectories. Final models of both wtTyk2 and P1104 (three for each) were obtained by cluster analysis of the last 40 ns of their corresponding MD trajectories. Cluster analysis used the *g_cluster* module of GROMACS and a backbone RMSD cut-off of 1 Å for two structures to be considered neighbors. The representative structure (structure with the smallest average RMSD from all other structures of a cluster) of each MD simulation was subsequently optimized by the steepest descent energy minimization with flexible water, to obtain the respective final MD models.

PyMOL (The PyMOL Molecular Graphics System, Version 1.7.0.0. Schrödinger, LLC) was used for visualization of trajectories and rendering of molecular model illustrations.

3 Results and discussion

Kinases are highly dynamic proteins and the structural flexibility and concerted motions in their kinase domains, are crucial for the allosteric regulation of the enzymatic activity of these proteins (Huse and Kuriyan, 2002; Kornev *et al.*, 2006; Kornev and Taylor, 2015).

To investigate the dynamics of the Tyk2 structure and the effect of the Pro1104 to Ala change on the structure and dynamics of this protein, we used MD simulations on the KDs of the wild type (wtTyk2) and the P1104A variant of Tyk2, respectively. Because of the stochastic nature of protein MD simulations and to reduce sampling problems, three independent MD simulations for each protein were carried out, and analyzed, as described in Section 2. The simulated systems had reached equilibrium and remained stable, at least, during the last 40 ns of the 100-ns trajectories in all cases and this simulation time range was subsequently used for the analyses of the MD trajectories.

3.1 Fluctuation analysis showed that the structure of the P1104A variant is overall less dynamic compared with wtTyk2

The flexibility of the structure of the two proteins under study was first assessed by means of RMSF analyses (see Section 2). The average backbone RMSF values of wtTyk2 and P1104A residues obtained from their corresponding sets of MD simulations, as well as the RMSF differences of P1104A relative to wtTyk2 along the sequence, are shown in Figure 2A and B, respectively.

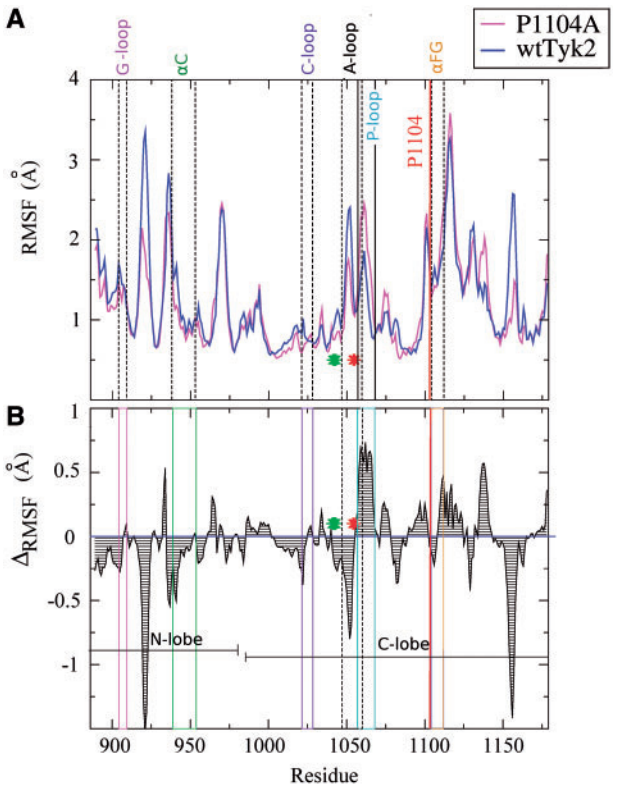

Fig. 2. Fluctuation analysis. **A**). Backbone RMSFs averaged within the respective sets of the three 100-ns MD trajectories of wtTyk2 and P1104A (see Section 2). **B**). Differences of the RMSF values shown in A, calculated from: Δ_{RMSF} = RMSF (P1104A) – RMSF (wtTyk2). Regions of the amino acid sequence corresponding to characteristic features of protein kinase domains, discussed in the text, are boxed and labeled (refer to Fig. 1, for comparison). Green and red asterisks denote the DFG motif, located just before the activation segment, and the Y1054–Y1055 regions, respectively

As shown in Figure 2, the P1104A variant, and especially its N-lobe and A-loop (bearing the Y1054-Y1055 site), is much less flexible compared with wtTyk2 (negative Δ_{RMSF} values, in Fig. 2B). These observations are better illustrated using coloring of the average MD structures by B-factor values of their backbone atoms obtained from the respective sets of MD simulations of the two proteins (see Section 2), shown in Figure 3. As indicated by low backbone B-factor values (in blue in Fig. 3), the P1104A variant was overall more rigid than wtTyk2.

On the contrary, the N-lobe and a large part of the C-lobe (including the A-loop), appeared to be much more dynamic in wtTyk2, as indicated by higher backbone RMSF (Fig. 2) and B-factor values of these regions (compare B-factor-based coloring in Fig. 3). Interestingly enough, the α_{FG} helix, bearing Pro1104/Ala1104 exhibited equally high fluctuations in both proteins (Figs 2 and 3). Taken together, these observations suggest that the Pro1104 to Ala substitution has long-range effects.

3.2 Cross-correlation analyses revealed a large disruption of correlated motions in the case of the P1104A protein

As already mentioned, concerted movements of various regions of kinase domains are necessary for the allosteric regulation of the

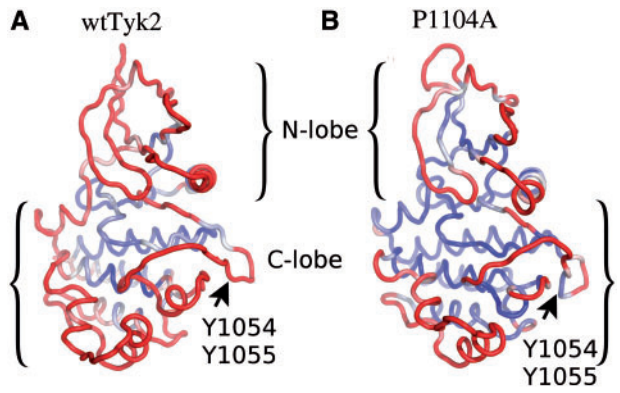

Fig. 3. B-factor-based color illustrations of ribbon models of the average MD structures of wtTyk2 (**A**) and P1104A (**B**), obtained from their corresponding concatenated MD trajectories. The color scaling according to backbone B-factor values (see Section 2) is from blue to red, for small (=low mean fluctuations; ≤0.6 Å) to large B-factor values (=high mean fluctuations; ≥1.3 Å), respectively. The orientation of the models is as in Figure 1, for comparisons

activity of protein kinases (Kornev and Taylor, 2015). To address this issue, we first used PCA analysis (see Section 2). Subsequent inspection of the animations of filtered configurations projected on the first eigenvectors (dominant modes of system's motions) produced by PCA analysis, revealed that the backbone atoms of wtTyk2 moved in a highly concerted manner along the corresponding MD trajectories, as opposed to the P1104A case.

To investigate this further, we calculated cross-correlation coefficients of the motions of the Cα atoms along the corresponding concatenated trajectories for both proteins (see Section 2). Correlation coefficients close to +1 or -1 indicate highly correlated motions (movements of atoms in the same and opposite directions, respectively), whereas correlation coefficients of 0 indicate uncorrelated movements. As shown in Figure 4, the motions of the Cα atoms of wtTyk2 were indeed highly correlated (both positively and negatively) along its concatenated MD trajectories (Fig. 4A and B, top panel). Interestingly enough, these networks of highly correlated Cα motions appeared to be largely disrupted in the case of the P1104A variant (Fig. 4, bottom panel), indicating that the P1104 to Ala replacement affects the communication between various parts of the KD of Tyk2. This, in turn, is expected to affect the catalytic status and the allosteric regulation of the activity of this protein.

3.3 Analyses of the MD results showed that the P1104A variant is stabilized in inactive and inadequate for phosphorylation of the activation segment, conformations

To investigate this hypothesis we focused our analyses on various structural features, characteristic of the activation status of protein kinases.

3.3.1 Relative movement of the N- and C-lobes

As indicated by high negative correlation coefficients between the movements of their Cα atoms, the N- and C-lobes of wtTyk2 moved in a concerted manner in opposite directions throughout its respective MD trajectories, whereas P1104A lacked such correlated motions (Fig. 4). Such movements are indicative of a switching between 'open' and 'closed' conformations of the active site cleft in the case of wtTyk2. This is better illustrated by the distribution of the angle describing the active site cleft, along the individual MD

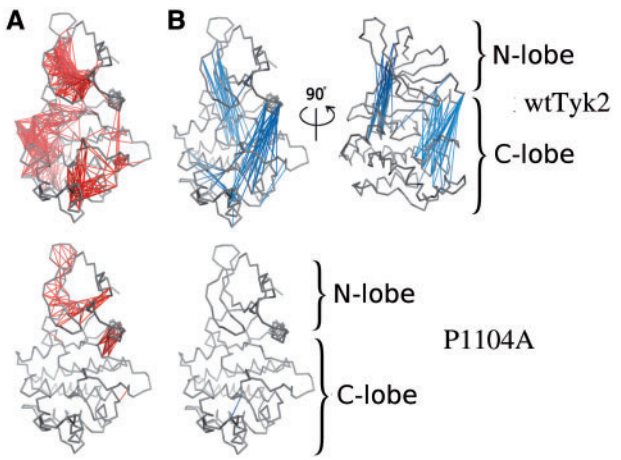

Fig. 4. Cross-correlation analysis of the motions of the Cα atoms over the course of the corresponding concatenated MD trajectories of wtTyk2 (upper panel) and P1104A (lower panel). Highly correlated residues (−0.7 ≤ correlation coefficients ≥ 0.7) (identified as described in Section 2) are interconnected by lines colored in red and blue, for positive and negative values of the correlation coefficients of the motions of their Cα atoms, respectively

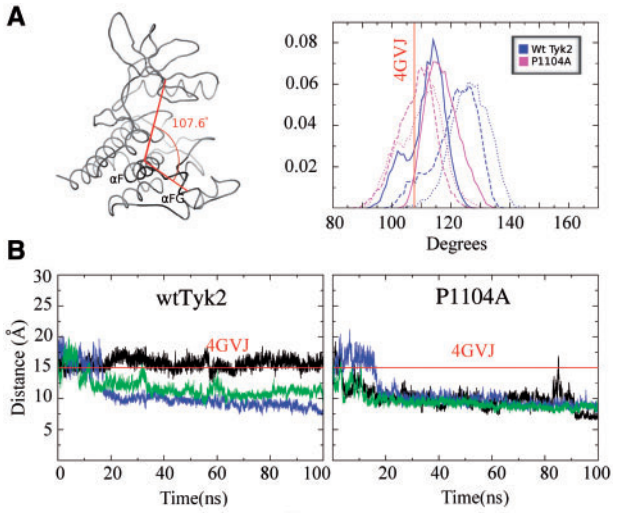

Fig. 5. (**A**) Distribution of the angle between the N- and C-lobes along the equivalent MD trajectories (three for each) for wtTyk2 and P1104A. The definition of the angle is shown on the left panel. The helix αF was chosen as pivot point because of its role as scaffold for the assembly of active protein kinases (Kornev *et al.*, 2008). (**B**) Monitoring of the distance between the G-loop and the catalytic loop (C-loop in Fig. 1) along the three 100-ns MD trajectories (in black, blue and green respectively) of wtTyk2 (left panel) and P1104A (right panel). Red lines indicate the respective N-C angle and distance in the case of the 4GVJ crystal structure

trajectories (Fig. 5A, left panel). As shown in Figure 5A (right panel), the P1104A variant appeared to adopt overall more 'closed' conformations, with angle values similar to that of the ADP-bound form of the protein (4GVJ PDB entry) used as initial conformation, in all three corresponding MD simulations. The wtTyk2, on the other hand, adopted more open conformations (rotations of two lobes by more than 10° relative to the starting conformation) with broader distributions of the corresponding angle (Fig. 5A, right panel). Such conformational mobility between the N- and C-lobes is essential for the catalytic activity of protein kinases (Kornev *et al.*, 2006), and its restriction (by the presence of the pseudokinase

domain) has been proposed to block the activation of Tyk2 (Lupardus *et al.*, 2014).

3.3.2 Distance between the G-loop and the catalytic loop

The distance between the G-loop and the catalytic-loop (C-loop) is another measure of the conformation of the active site of kinases. For example in the case of activated PKA kinase, MD simulations showed that this distance varied up to ∼18.3 Å (open) in the case of the apo-form but was reduced to ∼15.5 Å (closed) in its ATP-bound form (Li *et al.*, 2014). As shown in Figure 5B, this distance varied among the three MD simulations of wtTyk2 (Fig. 5B, left panel), but was reduced and remained constant at much smaller values (<10 Å) compared to 4GVJ, in all three corresponding MD simulations of the P1104A variant (Fig. 5B, right panel), indicating that the G- and C-loops remain constantly in close contact, in the case of the variant. The later observation indicates a persistent placement of the G-loop within the ATP-binding pocket, in P1104A, most probably blocking access of the ATP molecule and therefore hindering the catalytic activity of this variant. In line with this hypothesis, is the observation that the G-, C-loop distance has a similar value (∼9 Å) in the case of a crystal structure of wtTyk2 in complex with an ATP-competing inhibitor-compound bound into its ATP-binding pocket [PDB entry: 3NZ0 (Tsui *et al.*, 2011)].

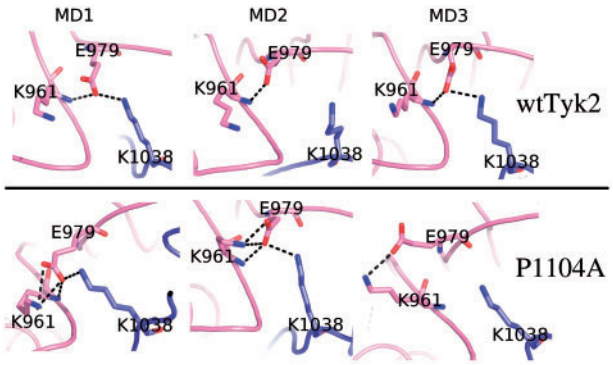

Fig. 6. The 'molecular break' region. Final models obtained from the corresponding MD simulations of wtTyk2 (upper panel) and P1104A (lower panel), focused on the region corresponding to the 'molecular break' (see text). The corresponding Tyk2 residues are labeled and shown as stick models. Hydrogen-bonds are shown with broken lines

3.3.3 The 'molecular break'

The notion of a 'molecular break' in their hinge region, regulating the activity of receptor tyrosine kinases, has been introduced by Chen *et al.* (2007). According to this idea, the formation of hydrogen-bonds between side-chain atoms of three residues on the back of the kinase domain restricts the, required for catalysis, relative motions between the N- and C-lobes of these kinases and is indicative of inactive conformations. The equivalent residues in Tyk2 are: K961, E979 and K1038 located at the N-lobe, hinge region and C-lobe, respectively. Hydrogen-bonds between side-chain atoms of these residues, reminiscent of the molecular break, were observed in two out of the three MD models of P1104A (Fig. 6, lower panel), whereas the situation was reversed in the case of wtTyk2 (Fig. 6, upper panel).

Taken together our observations so far suggest that, although the unphosphorylated wtTyk2, studied here, is able to explore various conformations, replacement of P1104 by Ala stabilizes mainly inactive conformations of this protein that block regulation of its activation.

3.3.4 The Y1054-Y1055 region

As already mentioned, activation of Tyk2 requires phosphorylation of tyrosines Y1054 and Y1055 (Gauzzi *et al.*, 1996), which are located at the end of its A-loop (amino acids: 1047–1060) and more precisely, at the beginning of a β-strand (β11), which is part of a β-sheet (β11–β12 sheet) in the 4GJV crystal structure (Liang *et al.*, 2013) (Fig. 1). As shown above (Figs 2 and 3), the segment of the A-loop at the site of Y1054–Y1055 was much less dynamic during the MD trajectories of the P1104A variant compared to wtTyk2 (compare RMSF differences and B-factor-based coloring of the Y1054-Y1055 region in Figs 2 and 3, respectively). To investigate these observations further, we performed secondary structure analyses. Monitoring of the secondary structure along the corresponding MD trajectories is shown in Figure 7.

As shown in Figure 7 (upper panel) the initial β11–β12 sheet structure (in red) was disrupted and an order-to-disorder (β-sheet to coil; red to white color, respectively) transition occurred in this region after the first 10 ns in two (MD2, MD3) out of three MD simulations of wtTyk2 (Fig. 7, upper panel). This observation, in conjunction with the importance of structural disorder in protein recognition and phosphorylation (Iakoucheva *et al.*, 2004), is in

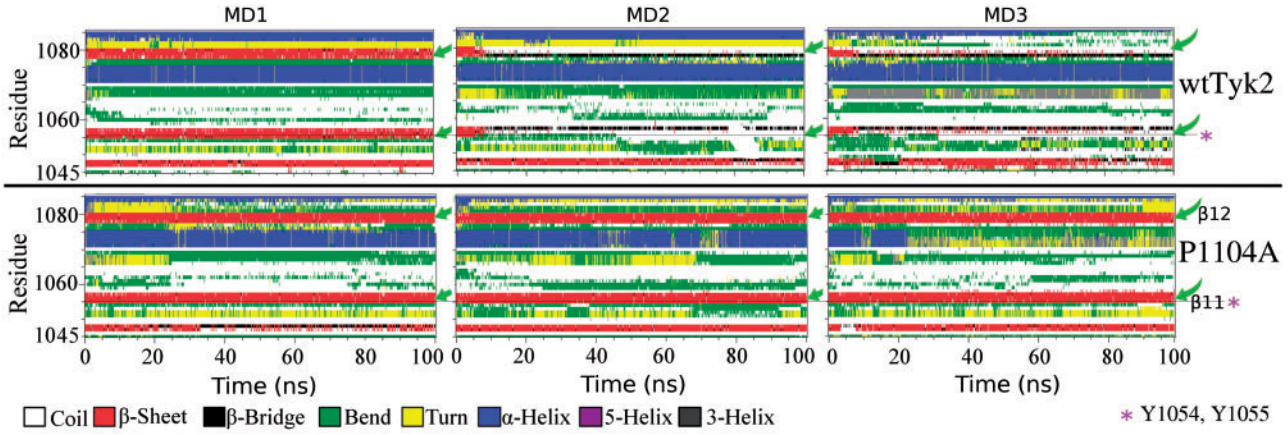

Fig. 7. Monitoring of the secondary structure along the equivalent sets of 100-ns MD trajectories of wtTyk2 (upper panel) and P1104A (lower panel). A color definition of secondary structure elements is shown at the bottom of the figure Green arrows point to the position of the initial β11–β12 sheet (see text). The Y1054–Y1055 region is indicated by asterisks, in magenta

perfect agreement with the ability of wtTyk2 to get phosphorylated at these tyrosines and therefore activated, as expected.

On the contrary, the β11–β12 sheet was preserved during all three MD simulations, in the case of P1104A (in red Fig. 7, bottom panel). This observation, in conjunction with low fluctuations of the region (Figs 2 and 3), suggests that, in contrast to wtTyk2, the activation segment of P1104A adopts conformations of the phosphosite (Y1054-Y1055) inadequate for phosphorylation, thus preventing activation of this variant. This hypothesis is in perfect agreement with experimental data showing reduced phosphorylation and enzymatic activity of Tyk2 to be associated with the rs34536443 polymorphism (Couturier *et al.*, 2011; Dendrou *et al.*, 2016; Tomasson *et al.*, 2008).

4 Conclusions

In this study we used molecular dynamics simulations to explore the structural consequences of the Pro1104 to Ala substitution, associated with the rs34536443 polymorphism of *TYK2* gene, on the resulting Tyk2 protein, and therefore its function.

Our MD results revealed that this single amino acid change has long-range effects that restrict the dynamics of the Tyk2 variant in favor of inactive conformations that most probably switch-off the activation process of this protein, thus blocking the regulation of its enzymatic activity and therefore the associated signal transduction. This hypothesis is in perfect agreement with previous studies linking reduced phosphorylation and enzymatic activity of Tyk2 and attenuated signal transduction with the rs34536443 polymorphism (Couturier *et al.*, 2011; Dendrou *et al.*, 2016; Tomasson *et al.*, 2008).

In total, the results presented here, are in line with the notion that reduced Tyk2 kinase activity may be the mechanism for protection against autoimmune diseases and add to knowledge in support of the idea of targeting Tyk2 and its pathways as a therapeutic approach against these diseases (Couturier *et al.*, 2011).

Funding

We (IB-A; NCSR 'Demokritos') acknowledge support of this work by the project 'Target Identification and Development of Novel Approaches for Health and Environmental Applications' (MIS 5002514) which is implemented under the Action for the Strategic Development on the Research and Technological Sectors, funded by the Operational Programme 'Competitiveness, Entrepreneurship and Innovation' (NSRF 2014–2020) and co-financed by Greece and the European Union (European Regional Development Fund).

Conflict of Interest: none declared.

References

Amadei,A. *et al.* (1993) Essential dynamics of proteins. *Proteins*, **17**, 412–425.

Berendsen,H. *et al.* (1987) The missing term in effective pair potentials. *J. Phys. Chem.*, **91**, 6269–6271.

Chen,H. *et al.* (2007) 'Molecular Brake' in the kinase hinge region regulates the activity of receptor tyrosine kinases. *Mol. Cell*, **27**, 717–730.

Couturier,N. *et al.* (2011) Tyrosine kinase 2 variant influences T lymphocyte polarization and multiple sclerosis susceptibility. *Brain*, **134**, 693–703.

Dendrou,C.A. *et al.* (2016) Resolving TYK2 locus genotype-to-phenotype differences in autoimmunity. *Sci. Transl. Med.*, **8**, 363ra149.

Diogo,D. *et al.* (2015) TYK2 protein-coding variants protect against rheumatoid arthritis and autoimmunity, with no evidence of major pleiotropic effects on non-autoimmune complex traits. *PLoS One*, **10**, e0122271.

Dyment,D.A. *et al.* (2012) Exome sequencing identifies a novel multiple sclerosis susceptibility variant in the TYK2 gene. *Neurology*, **79**, 406–411.

Gauzzi,M.C. *et al.* (1996) Interferon-a-dependent activation of Tyk2 requires phosphorylation of positive regulatory tyrosines by another kinase. *Biol. Chem.*, **271**, 20494–20500.

Hess,B. *et al.* (2008) GROMACS 4: algorithms for highly efficient, load-balanced, and scalable molecular simulation. *J. Chem. Theory Comput.*, **4**, 435–447.

Humphrey,W. *et al.* (1996) VMD – Visual Molecular Dynamics. *J. Mol. Graphics*, **14**, 33–38.

Huse,M. and Kuriyan,J. (2002) The conformational plasticity of protein kinases. *Cell*, **109**, 275–282.

Iakoucheva,L.M. *et al.* (2004) The importance of intrinsic disorder for protein phosphorylation. *Nucleic Acid Res.*, **32**, 1037–1049.

Kabsch,W. and Sander,C. (1983) Dictionary of orotein scondary structure: pattern recognition of hydrogen-bonded and geometrical features. *Biopolymers*, **22**, 2577–2637.

Kornev,A.P. *et al.* (2006) Surface comparison of active and inactive protein kinases identifies a conserved activation mechanism. *Proc. Natl. Acad. Sci. USA*, **103**, 17783–17788.

Kornev,A.P. *et al.* (2008) A helix scaffold or the assembly of active protein kinases. *Proc. Natl. Acad. Sci. USA*, **105**, 14377–14382.

Kornev,A.P. and Taylor,S. (2015) Dynamics-driven allostery in protein kinases. *Trends Biochem. Sci.*, **40**, 628–647.

Kyogoku,C. and Tsuchiya,N. (2007) A compass that points to lupus: genetic studies on type I interferon pathway. *Genes Immun.*, **8**, 445–455.

Langrish,C.L. *et al.* (2004) IL-12 and IL-23: master regulators of innate and adaptive immunity. *Immunol. Rev.*, **202**, 96–105.

Li,C. *et al.* (2014) Molecular dynamics studies on the positive cooperativity of the Kemptide substrate with protein kinase A induced by the ATP ligand. *J. Phys. Chem. B*, **118**, 1273–1287.

Liang,J. *et al.* (2013) Lead identification of novel and selective TYK2 inhibitors. *Eur. J. Med. Chem.*, **67**, 175–187.

Lindqvist,A.K. *et al.* (2000) A susceptibility locus for human systemic lupus erythematosus (hSLE1) on chromosome 2q. *J. Autoimmun.*, **14**, 169–178.

Lucet,I.S. *et al.* (2006) The structural basis of janus kinase 2 inhibition by a potent and specific pan-Janus kinase inhibitor. *Blood*, **107**, 176–183.

Lupardus,P.J. *et al.* (2014) Structure of the pseudokinase-kinase domains from protein kinase TYK2 reveals a mechanism for Janus kinase (JAK) autoinhibition. *Proc. Natl. Acad. Sci. USA*, **111**, 8025–8030.

Murray,P.J. (2007) The JAK-STAT signaling pathway: input and output integration. *J. Immunol.*, **178**, 2623–2629.

Myrthianou,E. *et al.* (2017) Investigation of the genetic overlap between Rheumatoid Arthritis and Psoriatic Arthritis in a Greek population. *Scand. J. Rheumatol.*, **46**, 180–186.

Oostenbrink,C. *et al.* (2004) A biomolecular force field based on the free enthalpy of hydration and solvation: the GROMOS force-field parameter sets 53A5 and 53A6. *J. Comput. Chem.*, **25**, 1656–1676.

Peluso,C. *et al.* (2013) TYK2 rs34536443 polymorphism is associated with a decreased susceptibility to endometriosis-related infertility. *Hum. Immunol.*, **74**, 93–97.

Shimoda,K. *et al.* (2000) Tyk2 plays a restricted role in IFN alpha signaling, although it is required for IL-12- mediated T cell function. *Immunity*, **13**, 561–571.

Tomasson,M.H. *et al.* (2008) Somatic mutations and germline sequence variants in the expressed tyrosine kinase genes of patients with de novo acute myeloid leukemia. *Blood*, **111**, 4797–4808.

Tsui,V. *et al.* (2011) A new regulatory switch in a JAK protein kinase. *Proteins*, **79**, 393–401.

Velazquez,L. *et al.* (1992) A protein tyrosine kinase in the interferon a/b signaling pathway. *Cell*, **70**, 313–322.

Voukkalis,N. *et al.* (2016) SRPK1 and Akt protein kinases phosphorylate the RS domain of Lamin B receptor with distinct specificity. *PLoS ONE*, **11**, e0154198.

Yamaoka,K. *et al.* (2004) The janus kinases (Jaks). *Genome Biol.*, **5**, 253.